ECCOMAS Congress 2016
VII European Congress on Computational Methods in Applied Sciences and Engineering
M. Papadrakakis, V. Papadopoulos, G. Stefanou, V. Plevris (eds.)
Crete Island, Greece, 5–10 June 2016

DESIGN OF ISOTROPIC MICROSTRUCTURES VIA A TWO-SCALE APPROACH

Alexis Faure[1], Georgios Michailidis[1], Rafael Estevez[1], Guillaume Parry[1] and Grégoire Allaire[2]

[1]SIMaP, INP Grenoble
1130 rue de la Piscine, Domaine universitaire BP75, 38402 Saint Martin d'Hères, France
e-mail: {alexis.faure,georgios.michailidis,Rafael.Estevez,guillaume.parry}@simap.grenoble-inp.fr

[2] Centre de Mathématiques Appliquées (CMAP), École Polytechnique
CNRS UMR 7641, Université Paris-Saclay, 91128 Palaiseau, France
e-mail: gregoire.allaire@polytechnique.fr

Keywords: Materials, homogenization, topology optimization, level-set.

Abstract. *Architectured materials are promising to reach extreme properties and ultimately address issues related to lightweight or non conventional properties for bulk materials (eg. high specific rigidity, extremal conductivity or auxetism (negative Poisson's ratio)) [1]. A very efficient way to obtain optimal forms is via inverse homogenization, i.e. using shape and topology optimization techniques in order to achieve target material properties [2].*

A great number of publications has been devoted to the design of isotropic materials with extreme properties. Isotropy is usually prescribed via a combination of symmetric planes and penalization techniques, which are quite delicate to handle in an optimization framework.

In this work, we present an approach for the design of isotropic multi-materials with extremal conductivity via laminate geometries, consisting in anisotropic phases [3]. More specifically, we design composites with extremal conductivity using rank-1 laminates, composed by two orthotropic phases along parallel layers. The second phase is obtained by a 90-degree rotation of the first one, while their volume fractions are explicitly chosen so that the laminate is isotropic. The orthotropic phases are considered to have their own periodic micro-structure, composed by multiple phases. By optimally distributing the different phases in a periodic cell, we can achieve the Hashin-Shtrikman bounds for the isotropic laminate. We present examples in two dimensions using the level-set method for shape and topology optimization [4].

1 INTRODUCTION

Designing materials with prescribed or extremal properties is of great interest in material science. Combining the different attributes of materials in nature, e.g. by designing properly their microstructure, one can create novel materials with mechanical properties that are not met by any material in nature alone (extreme conductivity, auxetism, etc.). This class of materials is frequently reffered to as *architectured* or *hybrid materials* [5, 6].

Among the different methodologies proposed for their design [7], the geometric approach has recently started attracting again the interest of reseachers and manufacturers. This is mainly due to the recent advances in additive manufacturing, which have rendered possible the realization of such materials, broadening the perspectives to fill the holes in the material property maps [7]. In this approach, the microstructure of the hybrid material, composed by multiple phases or one phase and void, is designed by specifying the exact configuration of its consituents in a periodic unit cell.

Beyond analytical solutions, based mainly on the experience and intuition of researchers [1], numerical methods for the design of architectured materials have been presented long ago. Using the theory of periodic homogenization [8, 9], it amounts to formulate an optimization problem where the homogenized coefficients appear and the design variables are chosen to describe the geometry and connectivity of the microstructure's shape [10, 11, 2, 12].

Among the different possibilities, the design of isotropic materials is of particular interest [13, 2, 14]. For such materials, explicit bounds for their effective homogenized properties have been derived and are used for validating the efficiency of the numerical methods to provide morphologies with extremal properties. However, ensuring numerically the isotropy of the microstructure is a computationally tedious task and often leads to complicated geometries. It is of interest to search for methods able to produce simpler geometries and requiring less numerical effort for imposing the isotropy conditions.

In this work, we propose to design isotropic architectured materials with extremal conductivity, using a two-scale approach [3, 15]. The isotropic material at the macroscale (scale 1) disposes a microstructure (scale ϵ), composed of periodic rank-1 laminates. The two materials forming the laminate are assumed orthotropic and to have their own microstructure (scale ϵ^2). More specifically, the second material is obtained from the first via a 90^o rotation, while their volume fraction at the scale ϵ is explicitly defined so that the global material is isotropic. The microstructure of the orthotropic materials is composed by one or mutliple phases, optimally distributed in a periodic unit cell such that the global laminate achieves the Hashin-Shtrikman bounds. Using the level-set method for Topology Optimization (T.O.) [4, 16], we present two-dimensional examples of microstructures achieving extremal conductivity.

2 SETTING OF THE PROBLEM

2.1 Two-scale approach

We search to design macroscopically isotropic materials with extreme conductivity coefficients. As aforementioned, the macroscopic material (see Figure 1,right) is assumed to be composed of periodic rank-1 laminates (see Figure 1,middle), with period $\epsilon << 1$. The laminate is formed by arranging two orthotropic phases in proportions f and $1-f$ correspondingly. The conductivity tensor of the first phase, in proportion f (see Figure 1,middle in orange colour) reads

$$A^0 = \begin{pmatrix} \alpha & 0 \\ 0 & \beta \end{pmatrix}, \quad \alpha, \beta > 0, \tag{1}$$

while the one of the second phase, in proportion $1-f$ (see Figure 1,middle in blue colour), denoted A^{90}, is derived by rotating A^0 by 90^o, i.e.

$$A^{90} = \begin{pmatrix} \beta & 0 \\ 0 & \alpha \end{pmatrix} = \Pi^t A^0 \Pi, \quad \text{where} \quad \Pi = \begin{pmatrix} 0 & 1 \\ -1 & 0 \end{pmatrix}. \tag{2}$$

The effective (homogenized) conductivity tensor A^* of the material at the macroscale reads

$$A^* = \begin{pmatrix} A^*_{11} & 0 \\ 0 & A^*_{22} \end{pmatrix}, \tag{3}$$

where its coefficients A^*_{11},A^*_{22} are analytically expressed as functions of f, α, β using classical lamination formulas [17, 18], as

$$A^*(f,\alpha,\beta) = \begin{pmatrix} \left(\frac{f}{\alpha} + \frac{1-f}{\beta}\right)^{-1} & 0 \\ 0 & f\beta + (1-f)\alpha \end{pmatrix}. \tag{4}$$

One can then easily verify that choosing the proportion of mixture f equal to

$$f = f(\alpha,\beta) = \frac{\sqrt{\alpha\beta} - \alpha}{\beta - \alpha}, \tag{5}$$

the homogenized tensor A^* becomes isotropic ($A^*_{11} = A^*_{22}$). In the particular case where $\alpha = \beta$, the laminate is isotropic independently of f. In this case, one can choose f as the limit of (5) when $\alpha \to \beta$, that is $f = 0.5$.

Remark 2.1. *The above method is generalized in three dimensions using rank-2 laminates constructed as in [3].*

Until now, we have considered the coefficients of the conductivity tensor A^0 to be constants. Assuming that the orthotropic material, used as constituent for the rank-1 laminate, disposes its own periodic microstructure at a scale $\epsilon^2 << \epsilon$ (see Figure 1,left), we search to optimally distribute one or multiple phases in a periodic unit cell Y in order to achieve extremal conductivity for the homogenized global conductivity matrix $A^*(f,\alpha,\beta)$. Therefore, the conductivity tensor A^0 and the global conductivity tensor A^* now read

$$A^0 = \begin{pmatrix} A^0_{11}(\Omega) & 0 \\ 0 & A^0_{22}(\Omega) \end{pmatrix}, \quad A^0_{11}(\Omega), A^0_{22}(\Omega) > 0,$$

and

$$A^*(f, A^0_{11}(\Omega), A^0_{11}(\Omega)) \equiv A^*(f,\Omega).$$

2.2 Optimization problem

For the sake of simplicity, we present the case where the unit cell Y is filled by a single phase, occupying a domain $\Omega \subset Y$. The extension to multiple phases has been thoroughly presented in [19, 20].

Furthermore, we assume that the scale $\epsilon^2 << \epsilon << 1$ remains sufficiently large compared to the atomistic scale, in order for the framework of continuum mechanics to remain valid for

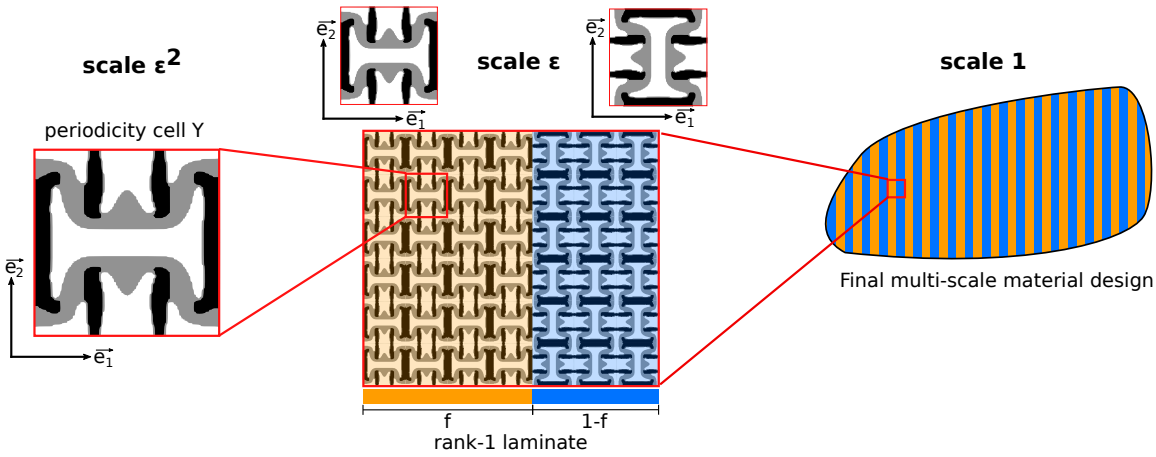

Figure 1: Two-scale approach for designing isotropic homogenized media.

our analysis. Then, the homogenized coefficients of the tensor $A^0(\Omega)$ are calculated using the formula

$$A^0_{ii} = \int_Y A(y)\,(e_i + \nabla_y w_i(y))\,(e_i + \nabla_y w_i(y))\,dy, \tag{6}$$

where w_i $(i = 1, 2)$ are solutions of the cell problems (see section 7.2.2 in [18])

$$\begin{cases} -\mathrm{div}_y\left(A(y)(e_i + \nabla_y w_i(y))\right) = 0 & \text{in Y} \\ y \to w_i(y) & \text{Y-periodic,} \end{cases} \tag{7}$$

e_i are vectors of the canonical Euclidean basis and $A(y)$ denotes the conductivity tensor of the consituent phases at $y \in Y$.

In order to design isotropic materials with extreme conductivity coefficients $A^*(f, \Omega)$, for a certain volume fraction of the consituent material, one can solve the optimization problem

$$\begin{aligned} \min_{\Omega} \quad & J(\Omega) = \pm tr(A^*(f,\Omega)) = \pm\left(A^*_{11}(f,\Omega) + A^*_{22}(f,\Omega)\right) \\ \text{s.t. :} \quad & A^*_{11}(f,\Omega) = A^*_{22}(f,\Omega) \\ & V(\Omega) = \alpha|Y|,\ \alpha \in (0,1), \end{aligned} \tag{8}$$

where the "+" and "-" signs correspond to design for minimal and maximal conductivity correspondingly.

3 TOPOLOGY OPTIMIZATION FRAMEWORK

In the framework of structural optimization, Topology Optimization refers to a form-finding method where the design variables are chosen to describe the shape and the connectivity of the structure. In general, a T.O. method is characterized by two main choices:

- a method to describe the shape and
- a method to evolve the shape during the optimization process.

Among the variety of T.O. developed during the last decades [21], we favor a geometric approach using the level-set method for the shape description, coupled with a shape sensitivity analysis for the shape advection [4]. The basic characteristics of the method are briefly presented in the following of this Section.

3.1 Level-set method

The level-set method, developped by Osher and Sethian [22], uses an implicit representation of an evolving front as the zero level-set of an auxiliary function ϕ. More precisely, assuming that the domain Ω of interest is a subset of a big working domain D, the level-set representation of Ω can be defined as (see Figure 2)

$$\begin{cases} \phi(x) = 0 & \leftrightarrow x \in \partial\Omega \cap D, \\ \phi(x) < 0 & \leftrightarrow x \in \Omega, \\ \phi(x) > 0 & \leftrightarrow x \in \left(D \setminus \overline{\Omega}\right), \end{cases} \tag{9}$$

A great benefit of the level-set representation for T.O. consists in performing topological

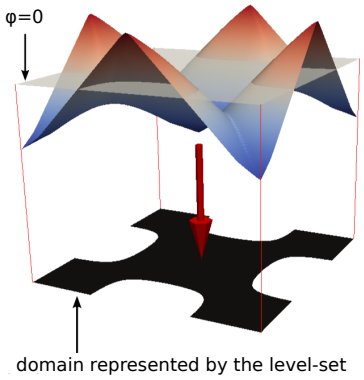

Figure 2: Level-set function representing a two-dimensional domain (in black).

changes with great ease and robustness, contrary to other methods using a parametrization for the shape description. Moreover, multiple phases can be described in a natural way [19, 23]. Defining n level-set functions in the same design domain and combining their values, one can describe up to $m = 2^n$ different materials (see Figure 3). The advection of a front (shape bound-

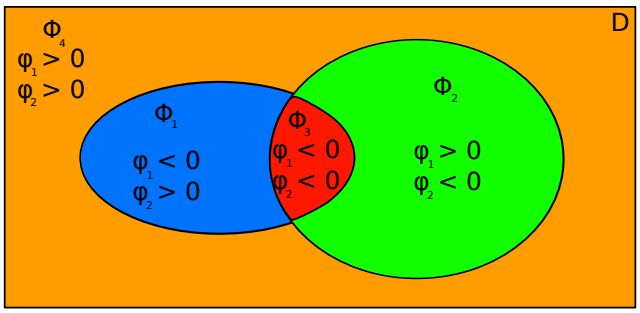

Figure 3: Multiphase representation in the level-set framework.

ary) with a velocity $V(x)$, normal to the shape boundary, is described in the level-set framework by introducing a pseudo-time, $t \in \mathbb{R}^+$, and solving the well-known Hamilton-Jacobi transport equation:

$$\frac{\partial \phi}{\partial t} + V(x)|\nabla \phi| = 0, \tag{10}$$

using an explicit second order upwind scheme [24], [25].

3.2 Shape sensitivity approach

In T.O. the velocity field $V(x)$ used for the shape evolution is chosen so that the objective function gets iteratively reduced. To employ a gradient-based optimization method, one needs to compute a derivative for the functionals involved in the optimization problem with respect to changes of the optimization parameters. However, no such parameters are a priori defined in the level-set framework. In [4], the authors proposed to derive such a descent direction via a classical shape sensitivity analysis. In this method, which dates back to Hadamard, a notion of **shape derivative**, i.e. a derivative of a functional with respect to variations of the shape in a direction $\theta(x) = V(x)n(x)$, can be defined as follows [18, 26].

Starting from a domain Ω, one considers perturbations by a smooth enough vector field $\theta(x)$, such that the new domain, Ω_θ, is described by (see Figure 4):

$$\Omega_\theta = \big(Id + \theta\big)\Omega.$$

Then, the shape derivative $J'(\Omega)(\theta)$ of the functional $J(\Omega)$ in a direction $\theta(x)$ is obtained

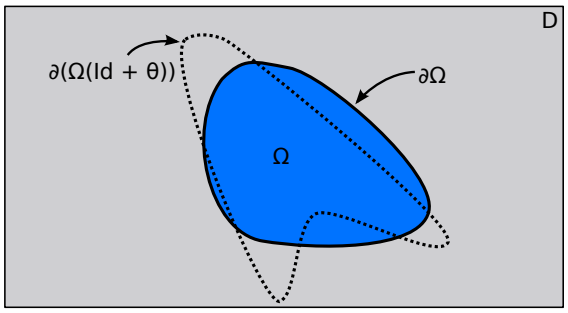

Figure 4: Perturbation of the domain Ω via a vector field $\theta(x)$.

through an asymptotic expansion formula of the type:

$$J\big((Id+\theta)\Omega\big) = J(\Omega) + J'(\Omega)(\theta) + o(\theta), \quad \text{with} \quad \lim_{\theta\to 0} \frac{|o(\theta)|}{\|\theta\|} = 0\ .$$

Once calculated, a descent direction can be found by advecting the shape in the direction $\theta = -tJ'(\Omega),\ t > 0$. For the new shape $\Omega_t = (\,\mathrm{Id} + t\theta)\,\Omega$, if $V \neq 0$, one can formally write:

$$J\left(\Omega_t\right) = J\left(\Omega\right) - t(J'(\Omega))^2 + \mathcal{O}(t^2) < J\left(\Omega\right),$$

which guarantees a descent direction for small positive t.

3.3 SHAPE DERIVATIVE

In this section, we compute a shape derivative for the objective function $J(\Omega)$ defined in (8). The isotropy constraint is treated by choosing f to satisfy the relation (5).

The shape derivative of $J(\Omega)$ reads

$$\begin{aligned} J'(\Omega)(\theta) &= \sum_{i=1}^{2} \pm \frac{\partial A_{ii}^*}{\partial \Omega}(\theta) \\ &= \sum_{i=1}^{2} \left[\sum_{j=1}^{2} \pm \frac{\partial A_{ii}^*}{\partial A_{jj}^0} \frac{\partial A_{jj}^0}{\partial \Omega}(\theta) \pm \frac{\partial A_{ii}^*}{\partial f} \frac{\partial f}{\partial A_{jj}^0} \frac{\partial A_{jj}^0}{\partial \Omega}(\theta) \right], \end{aligned} \tag{11}$$

where

$$\frac{\partial A^*_{11}}{\partial A^0_{11}} = \frac{(A^0_{22})^2 f}{(A^0_{22}f + (1-f)A^0_{11})^2} \quad , \quad \frac{\partial A^*_{11}}{\partial A^0_{22}} = \frac{(A^0_{11})^2 (1-f)}{(A^0_{22}f + (1-f)A^0_{11})^2}$$

$$\frac{\partial A^*_{22}}{\partial A^0_{11}} = (1-f) \quad , \quad \frac{\partial A^*_{22}}{\partial A^0_{22}} = f$$

$$\frac{\partial A^*_{11}}{\partial f} = \frac{-A^0_{11}A^0_{22}(A^0_{22} - A^0_{11})}{(A^0_{22}f + (1-f)A^0_{11})^2} \quad , \quad \frac{\partial A^*_{22}}{\partial f} = A^0_{22} - A^0_{11}$$

$$\frac{\partial f}{\partial A^0_{11}} = \frac{A^0_{22}(\sqrt{A^0_{11}} - \sqrt{A^0_{22}})^2}{2\sqrt{A^0_{11}A^0_{22}}(A^0_{22} - A^0_{11})^2} \quad , \quad \frac{\partial f}{\partial A^0_{22}} = \frac{-A^0_{11}(\sqrt{A^0_{11}} - \sqrt{A^0_{22}})^2}{2\sqrt{A^0_{11}A^0_{22}}(A^0_{22} - A^0_{11})^2}$$

and the shape derivative of the homogenized coefficients $\frac{\partial A^0_{jj}}{\partial \Omega}(\theta)$ are provided by the expression (see [27, 12])

$$\frac{\partial A^0_{jj}}{\partial \Omega}(\theta) = \int_{\partial\Omega} \theta(x) \cdot n(x) \left[A(x) \left(e_j + \nabla_y w_j(x) \right) \left(e_j + \nabla_y w_j(x) \right) \right] dx.$$

4 NUMERICAL RESULTS

In order to test the efficiency of the proposed methodology and algorithm, we compare our results with the Hashin-Shtrikman (HS) bounds [28, 29] for extremal conductivity coefficients of isotropic composites, using multiple isotropic phases. The lower (λ^l_{HS}) and upper (λ^u_{HS}) HS bounds read

$$\lambda^l_{HS} = -\min_i(\lambda_i) + \left[\sum_i \frac{V_i}{\lambda_i + \min_j(\lambda_j)} \right]^{-1} \tag{12}$$

and

$$\lambda^u_{HS} = -\max_i(\lambda_i) + \left[\sum_i \frac{V_i}{\lambda_i + \max_j(\lambda_j)} \right]^{-1} , \tag{13}$$

where V_i, λ_i the volume fraction and the thermal conductivity of the i^{th} phase, respectively.

For all our numerical results, we discretize both the level-set advection equation (10) and the cell problem (7) on a regular grid. For the cell problem Q1 finite elements have been used. The optimization problem (8) is solved using an SLP method.

4.1 Bi-material composites for minimal conductivity

In the first example, we design composites with minimal conductivity using two isotropic phases 1 and 2, with conductivity $\lambda_1 = 1$ and $\lambda_2 = 10$ respectively. Material 1 (in black colour) occupies domain Ω, while material 2 (in white colour) occupies the complementary of the periodic unit cell $Y \setminus \Omega$. The optimization problem reads

$$\begin{aligned} \min_{\Omega} \quad & J(\Omega) = tr(A^*(f,\Omega)) = (A^*_{11}(f,\Omega) + A^*_{22}(f,\Omega)) \\ \text{s.t. :} \quad & A^*_{11}(f,\Omega) = A^*_{22}(f,\Omega) \\ & V(\Omega) = 0.5|Y|. \end{aligned} \tag{14}$$

The HS lower bound for this case equals $\lambda^l_{HS} = 2.385$.

In Figure 5 we see two optimized shapes (right column) for two different initializations (left column). For the first result (upper row), the homogenized conductivity coefficients A^*_{ii} equal 2.588, while the volume fraction of laminate A^0 equals $f = 0.5$. For the second result (lower row), the homogenized conductivity coefficients A^*_{ii} equal 2.433 and the volume fraction of laminate A^0 equals $f = 0.506$.

As expected, in both results the less conductive material (in black) "encapsulates" the highly conductive phase (in white), leading to a composite with effective conductivity close to the HS bounds.

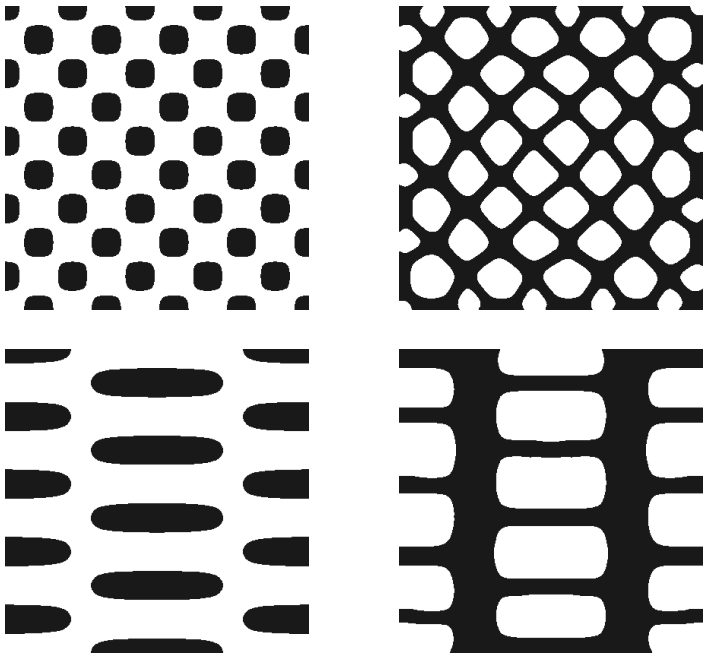

Figure 5: Bi-material design for minimal conductivity; initializations (left) and resulting optimal shapes (right).

4.2 Three-phase composites for maximal conductivity

In the second example, we design composites with maximal conductivity using three isotropic phases 1, 2 and 3, with conductivity $\lambda_1 = 10$, $\lambda_2 = 2$ and $\lambda_3 = 1$. Materials 1 and 2, in red and white colour respectively, occupy domains Ω_1 and Ω_2, while material 3 (in blue colour) occupies the complementary of the periodic unit cell. The optimization problem reads

$$\begin{aligned} \min_{\Omega_i} \quad & J(\Omega_i) = -tr(A^*(f,\Omega_i)) = -\left(A^*_{11}(f,\Omega_i) + A^*_{22}(f,\Omega_i)\right) \\ \text{s.t. :} \quad & A^*_{11}(f,\Omega_i) = A^*_{22}(f,\Omega_i) \\ & V(\Omega_i) = V_i,\ i = 1,2,3. \end{aligned} \tag{15}$$

In Figure 6, we show different optimized shapes for various combinations of volume fractions for the three constitutive phases. The values of the homogenized coefficients appear in Table 1 and are compared both with the upper HS bounds λ^u_{HS}, as well as with results obtained by Zhou et al. in [29].

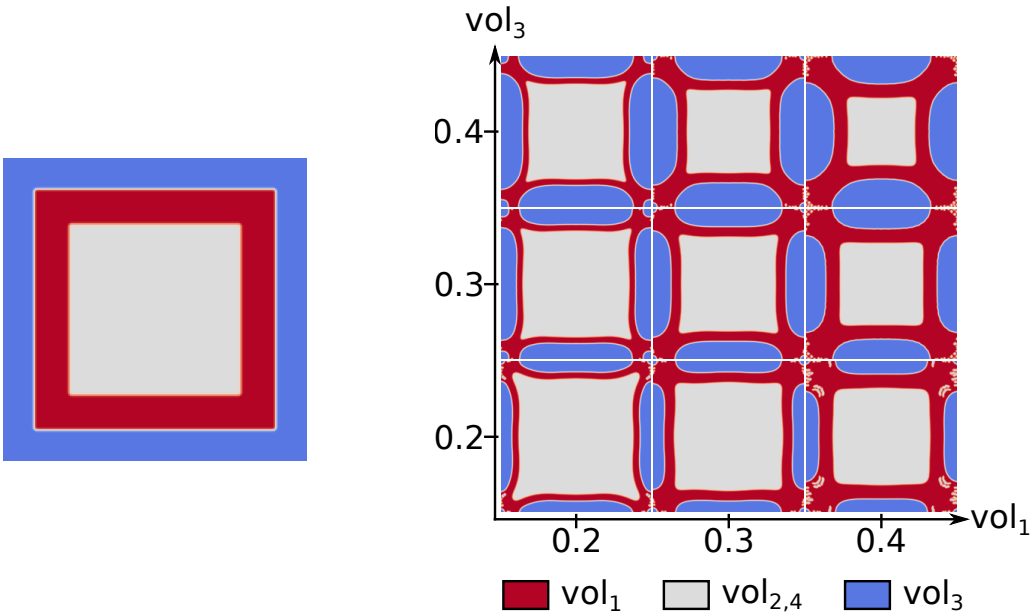

Figure 6: Initialization (left) and optimized shapes (right) for different volume fractions in the unit periodic cell Y.

Case	V_1	V_3	λ_1	λ_2	λ_3	λ^u_{HS}	λ_{Zhou}	A^*_{ii}
a	0.2	0.2	10	2	1	2.791	—	2.803
b	0.2	0.3	10	2	1	2.668	—	2.671
c	0.2	0.4	10	2	1	2.548	2.501	2.554
d	0.3	0.2	10	2	1	3.360	—	3.367
e	0.3	0.3	10	2	1	3.226	—	3.241
f	0.3	0.4	10	2	1	3.095	—	3.110
g	0.4	0.2	10	2	1	3.983	3.903	4.017
h	0.4	0.3	10	2	1	3.836	—	3.857
i	0.4	0.4	10	2	1	3.693	—	3.716

Table 1: Results of the optimized shapes of Figure 6.

Remark 4.1. *We shall note that the overpass of the HS bounds that appears in Table 1 is purely numerical. In fact, using the multi-material setting in [19], the volume of each phase is calculated approximatively, using the same smooth interpolation functions as for the mechanical properties. Reducing the interpolation width, the results converge to the HS bounds.*

As expected, starting from different initializations, one may obtain different optimized shapes. In Figure 7(right), we show the optimized shape for the case (c) in Table 1, starting from the initialization shown in Figure 7(left). The value of the homogenized coefficients is similar to Table 1(c) and equals 2.580. Similarly, starting from different initializations for the case (g) in Table 1, the optimized shapes are shown in Figure 8, where a repetition of the same pattern is observed. For all the results of this section, a cubic symmetry is observed, which leads to a volume fraction of $f = 0.5$ for the laminate A^0 at scale ϵ.

5 CONCLUSION

A novel method, at least to our knowledge, for the design of isotropic composites using T.O. has been proposed, based on a two-scale approach. The method has been applied for the

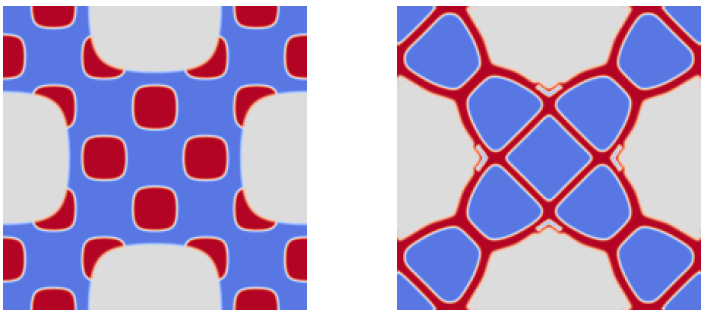

Figure 7: Initialization (left) and optimized shapes (right) for the case (c) in Table 1, starting from a different initialization.

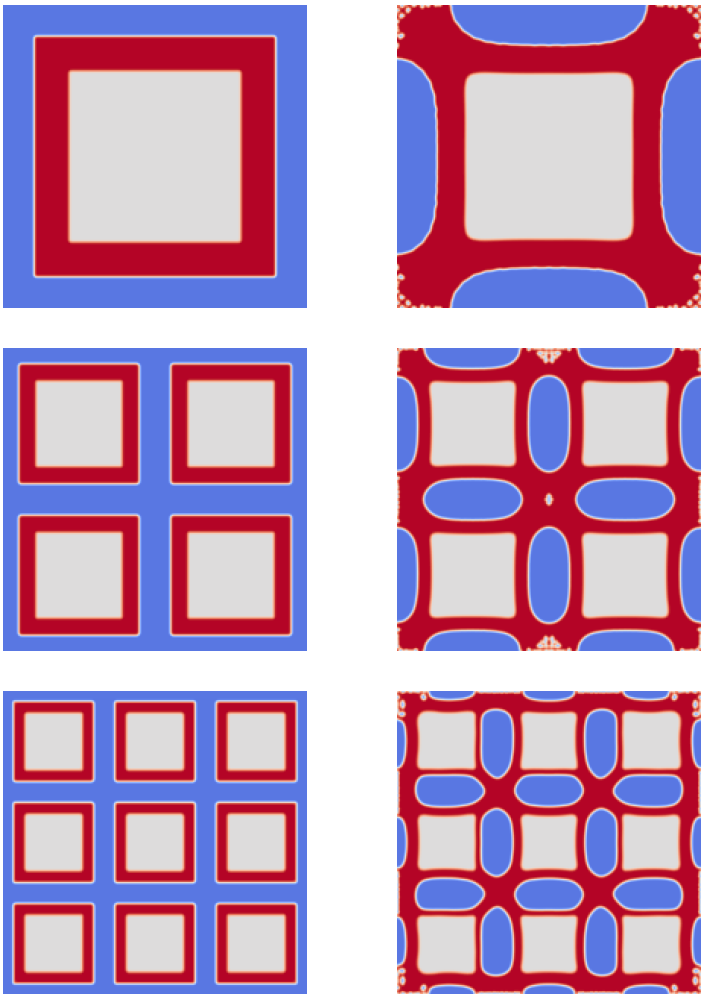

Figure 8: Initializations (left) and optimized shapes (right) for the case (g) in Table 1, starting from a different initializations.

design of architectured multi-materials with extremal conductivity, using the level-set method for Topology Optimization. The obtained results are very close to the HS bounds. Future work shall include three-dimensional results as well as the elasticity framework, aiming to obtain extremal micro-structures with simpler geometry.

REFERENCES

[1] G. Jefferson, T. Parthasarathy, and R. Kerans, "Tailorable thermal expansion hybrid structures," *International Journal of Solids and Structures*, vol. 46, no. 11, pp. 2372–2387, 2009.

[2] O. Sigmund, "Tailoring materials with prescribed elastic properties," *Mechanics of Materials*, vol. 20, no. 4, pp. 351–368, 1995.

[3] M. Avellaneda and G. Milton, "Optimal bounds on the effective bulk modulus of polycrystals," *SIAM Journal on Applied Mathematics*, vol. 49, no. 3, pp. 824–837, 1989.

[4] G. Allaire, F. Jouve, and A.-M. Toader, "Structural optimization using sensitivity analysis and a level-set method," *Journal of computational physics*, vol. 194, no. 1, pp. 363–393, 2004.

[5] M. Ashby, "Designing architectured materials," *Scripta Materialia*, vol. 68, no. 1, pp. 4–7, 2013.

[6] M. Ashby and Y. Brechet, "Designing hybrid materials," *Acta materialia*, vol. 51, no. 19, pp. 5801–5821, 2003.

[7] M. Ashby, "Hybrids to fill holes in material property space," *Philosophical Magazine*, vol. 85, no. 26-27, pp. 3235–3257, 2005.

[8] F. Murat and L. Tartar, "Calcul des variations et homogénéisation," *Les méthodes de lhomogénéisation: théorie et applications en physique*, no. 57, pp. 319–369, 1985.

[9] L. Tartar, *The general theory of homogenization: a personalized introduction*, vol. 7. Springer, 2009.

[10] G. Allaire, E. Bonnetier, G. Francfort, and F. Jouve, "Shape optimization by the homogenization method," *Numerische Mathematik*, vol. 76, no. 1, pp. 27–68, 1997.

[11] M. Bendsøe and N. Kikuchi, "Generating optimal topologies in structural design using a homogenization method," *Computer methods in applied mechanics and engineering*, vol. 71, no. 2, pp. 197–224, 1988.

[12] M. Wang and X. Wang, "A level-set based variational method for design and optimization of heterogeneous objects," *Computer-Aided Design*, vol. 37, no. 3, pp. 321–337, 2005.

[13] E. Andreassen, B. Lazarov, and O. Sigmund, "Design of manufacturable 3d extremal elastic microstructure," *Mechanics of Materials*, vol. 69, no. 1, pp. 1–10, 2014.

[14] O. Sigmund, "A new class of extremal composites," *Journal of the Mechanics and Physics of Solids*, vol. 48, no. 2, pp. 397–428, 2000.

[15] G. Milton, *The theory of composites*, vol. 6. Cambridge University Press, 2002.

[16] M. Wang, X. Wang, and D. Guo, "A level set method for structural topology optimization," *Computer methods in applied mechanics and engineering*, vol. 192, no. 1, pp. 227–246, 2003.

[17] G. Allaire, *Shape optimization by the homogenization method*, vol. 146 of *Applied Mathematical Sciences*. Springer-Verlag, New York, 2002.

[18] G. Allaire, *Conception optimale de structures*, vol. 58 of *Mathématiques & Applications (Berlin)*. Springer-Verlag, Berlin, 2007.

[19] G. Allaire, C. Dapogny, G. Delgado, and G. Michailidis, "Mutli-phase structural optimization via a level-set method," *ESAIM: Control, Optimisation and Calculus of Variations, 20, pp 576-611. doi:10.1051/cocv/2013076*, 2014.

[20] N. Vermaak, G. Michailidis, G. Parry, R. Estevez, Y. Brechet, and G. Allaire, "Material interface effects on the topology optimization of multi-phase thermoelastic structures using a level set method," *(submitted in SMO: Structural and Multi-disciplinary Optimization)*, 2013.

[21] M. Bendsoe and O. Sigmund, *Topology optimization: theory, methods and applications*. Springer, 2004.

[22] S. Osher and J. Sethian, "Fronts propagating with curvature-dependent speed: algorithms based on hamilton-jacobi formulations," *Journal of computational physics*, vol. 79, no. 1, pp. 12–49, 1988.

[23] M. Wang and X. Wang, "Color level sets: a multi-phase method for structural topology optimization with multiple materials," *Computer Methods in Applied Mechanics and Engineering*, vol. 193, no. 6, pp. 469–496, 2004.

[24] S. Osher and R. Fedkiw, *Level set methods and dynamic implicit surfaces*, vol. 153 of *Applied Mathematical Sciences*. Springer-Verlag, New York, 2003.

[25] J. Sethian, *Level set methods and fast marching methods: evolving interfaces in computational geometry, fluid mechanics, computer vision, and materials science*. Cambridge university press, 1999.

[26] J. Simon and F. Murat, "Sur le contrôle par un domaine géométrique," *Publication 76015 du Laboratoire d'Analyse Numérique de l'Université Paris VI*, no. 76015, p. 222 pages, 1976.

[27] G. Michailidis, *Manufacturing Constraints and Multi-Phase Shape and Topology Optimization via a Level-Set Method*. PhD thesis, Ecole Polytechnique X, 2014, available at: http://pastel.archives-ouvertes.fr/pastel-00937306.

[28] A. Cherkaev, "Bounds for effective properties of multimaterial two-dimensional conducting composites," *Mechanics of Materials*, vol. 41, no. 4, pp. 411–433, 2009.

[29] S. Zhou and Q. Li, "Computational design of multi-phase microstructural materials for extremal conductivity," *Computational Materials Science*, vol. 43, no. 3, pp. 549–564, 2008.